JOURNAL OF THEORETICAL AND APPLIED MECHANICS
45, 4, pp. 893-917, Warsaw 2007

EXPERIMENTAL STUDY OF VIBRATION CONTROL OF A CABLE WITH AN ATTACHED MR DAMPER

Marcin Maślanka
Bogdan Sapiński

AGH University of Science and Technology, Department of Process Control, Cracow, Poland
e-mail: masmar@agh.edu.pl; deep@agh.edu.pl

Jacek Snamina

Cracow University of Technology, Institute of Applied Mechanics, Cracow, Poland
e-mail: js@mech.pk.edu.pl

The paper presents experimental investigation of a horizontally suspended cable with an MR damper attached transversally near the support. The algorithm proposed to MR damper control employs the concept of emulation of a viscous damper with an optimal viscous damping coefficient. The algorithm is realized using a velocity feedback with damping force tracking control is applied. Free vibration of the cable with an MR damper operating in passive and controlled modes are investigated. The obtained results indicate that an appropriately controlled MR damper ensures a nearly constant damping level in a wide range of cable vibration amplitudes.

Key words: cable vibration, magnetorheological (MR) damper, control

1. Introduction

Since the 1960s, numerous cable-stayed bridges have been built all over the world, their spans and cables made longer and longer. In the early 1990s, the Skarnsund Bridge was opened – the first cable-stayed bridge with the main span length exceeding 500 m (Norway, 1991, main span 530 m). Other outstanding achievements of the 1990s include: Yang Pu Bridge (China, 1993, main span 602 m), Normandie Bridge (France, 1994, main span 856 m), Tatara Bridge (Japan, 1999, main span 890 m). They are light structures, constructed

with the use of state-of-the-art technologies (Virlogeux, 1999). These structures, particularly cables, are susceptible to vibration mainly due to weather conditions because of their low internal damping, relatively small mass, large flexibility and considerable length. Dangerous, high-amplitude cable vibrations caused serious damages.

Cable vibrations in cable-stayed bridges have received a great deal of attention recently. Many research teams study the complex nature of these vibrations and explore potential mitigating measures. Major research achievements were reported e.g. in (Kumarasena *et al.*, 2005; Virlogeux, 2005) and in international conference proceedings (AIM, 2005; MoDOT, 2006).

Most cable vibrations are induced by specific rain and wind interactions. Such vibrations were first recognised on the Meiko-Nishi Bridge in Japan (Hikami and Shiraishi, 1988). They occur in conditions of light to moderate winds $(5, 15)$ m/s and light rain. These rain-wind induced cable vibrations usually take form of one of several first natural cable modes, with the frequency range $(1, 3)$ Hz, and maximum amplitude approaching 1 m (Kumarasena *et al.*, 2005).

Reported are cable vibrations with larger amplitudes, too. One of the most intensive cable vibrations were registered on the Oresund Bridge, linking Denmark and Sweden, during severe snow storms. These vibrations might have been caused by wet snow accumulating on the cable surface. The registered amplitude of cable vibrations approached 3 m, the cable kept on vibrating for over an hour (Larsen and Lafreniére, 2005). In similar weather conditions, violent cable vibrations were observed twice on the Dubrovnik Bridge in Croatia, which damaged the cable protective sheathing and some anchoring elements (Savor *et al.*, 2006).

To mitigate cable vibrations, external viscous dampers are often attached to cables near lower anchorages (Persoon and Noorlander, 1999; Main and Jones, 2001) – the main purpose is to improve cable damping. In order to ensure the required damping level, viscous dampers should be carefully tuned, individually for each cable and each vibration mode to be damped. Too low external damping will not guarantee a sufficient cable damping level, whilst too high value shall cause the cable to be supported at the location of the damper which results in cable vibration with slightly increased frequency and no appreciable damping effect (Krenk, 2000). In practice, it is difficult to determine *a priori* the dominant vibration mode to which the viscous damper should be tuned. In specific weather conditions, the dominant mode might be different for individual cables. The occurrence of a specific cable vibration mode strongly depends also on the type of excitations.

It has to be emphasised that the longer the cables, the more difficult their vibration damping. The current expertise allows for construction of cable-stayed bridges with the main span length exceeding 1000 m and the cable length of 550 m. There are so large bridges under construction: Stonecutters Bridge (Hong Kong, to be commissioned in 2008, main span length 1018 m, maximal cable length 536 m) and Sutong Bridge (China, to be commissioned in 2009, main span 1088 m, maximal cable length 577 m). For practical reasons, external dampers are attached to cables at the distance of 1-2% of their length from the lower anchorage, which limits the capability of effective damping. Thus, precise tuning of dampers is of primary importance. New solutions are sought as e.g. those utilising MR dampers attached to cables in a similar manner as viscous dampers. The benefit of MR dampers is that their damping characteristic can be easily adapted to particular conditions.

The concept of using MR dampers in cable vibration reduction systems has received a great deal of attention. Applications of controlled semi-active elements to cable vibration control were first explored by Johnson *et al.* (1999, 2000). Their research focused on the taut string model and an ideal semi-active element (with no limitation on the maximum force). Simulation tests confirmed good performance of a sub-optimal (with passive constraints) LQ controller. Further tests were run on a model of a inclined cable, where cable sag was taken into account (Johnson *et al.*, 2003). Experimental verification was conducted in (Christenson *et al.*, 2001) on a laboratory cable model, 12.6 m in length.

A pioneering implementation of MR dampers to cable vibration control systems took place in 2002, on the Dongting Lake Bridge in China (Chen *et al.*, 2003; Duan *et al.*, 2006). Those dampers operated in the passive mode (under constant current). In this case, the MR damper force depends on the piston velocity in a minor degree only, which seems to be a major drawback. MR dampers capabilities can be fully utilised in the controlled mode of operation, provided an appropriate control algorithm is selected. The study of a control algorithm with experimental verification on the Dongting Lake Bridge was reported by Duan *et al.* (2005).

Research on semi-active vibration control systems complete with MR dampers was undertaken by other research teams, too. Results of experiments run on a horizontally suspended cable 215 m in length (a prototype cable for the Sutong Bridge) were compiled in (Sun *et al.*, 2004; Zhou and Sun, 2005). In those experiments, the performance of MR dampers operating in the passive mode were compared with the performance of other types of dampers.

Results of experiments on a cable 15.5 m in length were summarised by Weber *et al.* (2005c,d). This program was further pursued in the implementa-

tion of a single MR damper on the Eiland Bridge in the Netherlands (Weber *et al.*, 2005b). The tests were run on a specially designed and fabricated MR damper, generating a force up to 40 kN. This type of damper was utilised in 2006 on the Dubrovnik Bridge to counteract high-amplitude cable vibrations previously observed on this bridge (EMPA, 2006). That was the first implementation of a semi-active vibration control system on a cable-stayed bridge world-wide, utilising specially designed and controlled MR dampers.

This study summarises the experimental data gathered during laboratory tests of a cable 30 m in length. Both passive and controlled modes of MR damper operation are considered. The algorithm chosen for control purposes is that proposed by Weber *et al.* (2005a), which was first tested on the Eiland Bridge. The purpose of the tests was to explore potential applications of MR dampers operating in the passive mode to the cable vibration control and to find advantages of the applied control algorithm. Damping of cable vibrations using MR dampers both in passive and controlled modes is investigated thoroughly.

The article is organized as follows. Section 1 provides an introduction to the cable vibration problem and mitigation countermeasures, particularly using MR dampers. The considered cable-MR system is described in Section 2. Section 3 presents simple and inverse models of the MR damper. Section 4 deals with implementation of the control algorithm. Selected results are compiled in Section 5. Results obtained for cable vibration reduction systems complete with the controlled MR damper are preceded by the analysis of dynamic behaviour of the cable with the MR damper in the passive mode and the cable with no damper. Discussion of results and conclusions are provided in Sections 6 and 7.

2. System description

Of particular interest is a horizontally suspended and stretched cable of the length L, linear density m and static tension force T, with an MR damper attached transversely to the cable at the distance x_d from the support (Fig. 1). The main research area covers vibration control algorithms for this system.

The work by Krenk (2000) gives an approximate formula to determine the optimal viscous damping coefficient c_{opt} of a viscous damper attached to the cable at the point x_d, at a small distance from the support

$$c_{opt}^{n} = \frac{1}{n\pi}\frac{L}{x_d}\sqrt{Tm} \tag{2.1}$$

where: n – mode number.

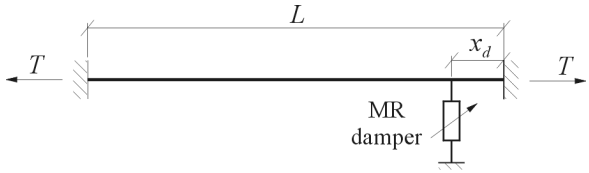

Fig. 1. Cable with an attached MR damper

The optimal value of the viscous damping coefficient for a cable with specified parameters and for the given damper location is different for each mode. As stated in Section 1, a viscous damper optimally tuned to damp one mode of vibrations may not optimally damp other modes. For a given cable and specific weather conditions, it is difficult to determine the dominant vibration mode to accurately tune the damper.

Capability of tuning of an MR damper to the occurring vibration mode proves to be its major advantage over conventional viscous dampers. When the appropriate control algorithm is chosen, one MR damper generating a sufficient force might be well utilised to damp several modes of vibrations of cables differing in lengths and with variable damper locations.

3. MR damper

MR dampers are controllable, semi-active actuators utilising MR fluids in their operation (Jolly *et al.*, 1999; Goncalves *et al.*, 2006). MR fluids have a property to reversibly change from the liquid to semi-solid state, in a continuous manner, under the action of a magnetic field.

The damper used for the purpose of the research program is an MR damper series RD-1097-01 (Lord Co., 2002). Its construction is different from typical linear stroke dampers filled with MR fluids and operating in the valve mode. The main difference lies in the presence of an absorbent matrix saturated with an MR fluid in the RD-1097-01 damper (Carlson, 1999; Chrzan and Carlson, 2001). A schematic diagram of the damper is shown in Fig. 2.

The key functional parameters of the damper RD-1097-01 listed by the manufacturer are: maximum force 100 N (for current 1 A and piston velocity 51 mm/s), stroke ± 25 mm, response time < 25 ms (time required to reach 90% of the steady-state value of force under a step change of the current from 0 to 1 A, for 51 mm/s). The force in the passive-off mode (0 A) is less than 9 N (at piston velocity 200 mm/s).

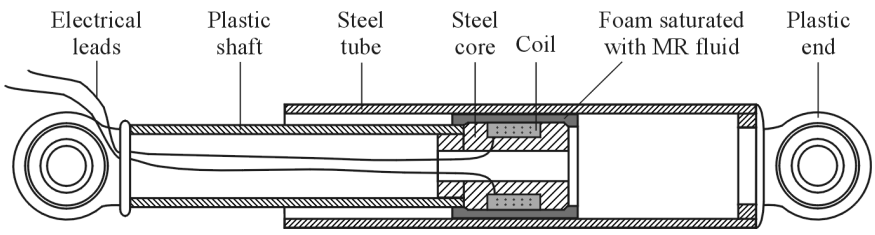

Fig. 2. Structure of the RD-1097-01 damper

The damper RD-1097-01 was first utilised in a cable vibration control system in laboratory tests run on a cable 7.2 m in length (Wu and Cai, 2006).

3.1. Visco-plastic model with hysteresis

An MR damper may be approximately considered as a friction damper with an additional force component proportional to velocity (viscous component). Accordingly, in steady state motion, the restoring force F_d of the MR damper is governed by the Bingham model (Spencer *et al.*, 1997)

$$F_d = F_c \operatorname{sgn}(\dot{w}_d) + c_0 \dot{w}_d \tag{3.1}$$

where: F_c is the friction force, $\dot{w}_d$ is the piston velocity and c_0 is the viscous damping coefficient.

The Bingham model accurately approximates the steady-state relationship between the restoring force and relative velocity of the piston in the MR fluid post-yield region ($|F_d| \geqslant F_c$). The model fails to capture the real nature of the damper restoring force in the pre-yield region ($|F_d| < F_c$), in which the MR fluid exhibits features of a quasi-solid body (Gandhi and Bullough, 2005).

In order to better fit the model to experimental data in the pre-yield region, the signum function in Eq. (3.1) is replaced by a hyperbolic tangent function (Guo *et al.*, 2006; Kwok *et al.*, 2006), and a hysteresis is added to the model

$$F_d = F_c \tanh[\mu(\dot{w}_d + p w_d)] + c_0(\dot{w}_d + p w_d) \tag{3.2}$$

where: μ is the scaling parameter enabling representation of smooth transition in the pre-yield region from negative to positive velocities and the other way round, p denotes the scaling parameter of the hysteresis. In the general case, the model parameters are functions of the current applied to the damper. For parameters $p = 0$, $\mu \to \infty$, the model governed by Eq. (3.2) is reduced to the Bingham model.

Identification of the model given by Eq. (3.2) is performed on the basis of experimental data. The design of the laboratory setup is described in more detail in the Subsection 5.1.

Figure 3 shows the results of model identification obtained by methods of parameter optimisation. Relationships between the parameters F_c and c_0 and the current I are approximated by linear functions

$$F_c = C_1 I + C_2 \qquad c_0 = C_3 I + C_4$$

where: $C_1 = 62\,\mathrm{N/A}$, $C_2 = 1.5\,\mathrm{N}$, $C_3 = 48\,\mathrm{Ns/Am}$, $C_4 = 14\,\mathrm{Ns/m}$. The remaining model parameters are: $\mu = 130\ \mathrm{s/m}$, $p = 1\ \mathrm{s}^{-1}$.

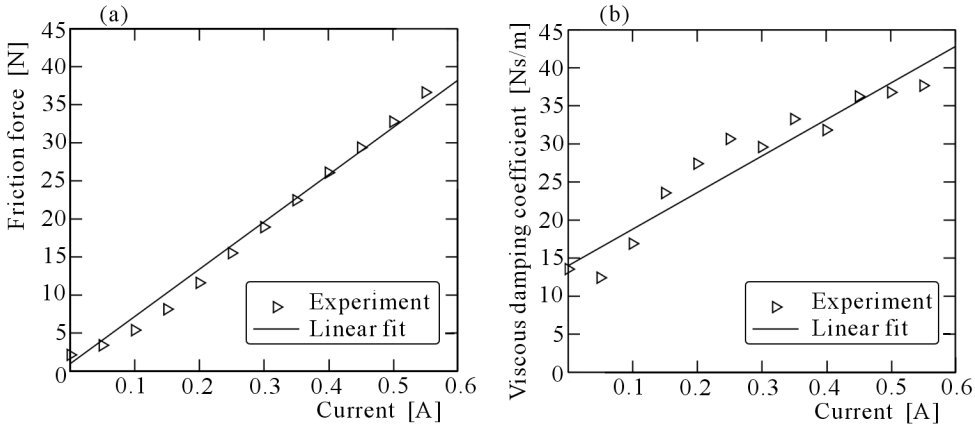

Fig. 3. Parameters of the MR damper model vs. current: (a) friction force (F_c), (b) viscous damping coefficient (c_0)

3.2. Inverse model

Realization of MR damper force tracking control systems often utilise an inverse model of MR dampers (Xia, 2003; Du *et al.*, 2005; Tsang *et al.*, 2006). In practical implementations of digital control systems, an inverse model may be represented by look-up-table based on the steady-state relationship between the current, damper force and piston velocity. An inverse model, formulated analytically, has a number of advantages, though it is difficult to obtain. The approach used here involves a linear approximation of relationships between model parameters and current (Fig. 3).

Assuming the approximating functions of model parameters, an inverse form of the presented model (Eq. (3.2)) is developed by direct transformations yielding the following equation (for $\dot{w}_d \neq 0$)

$$I = \frac{F_d - C_2 \tanh[\mu(\dot{w}_d + p w_d)] - C_4(\dot{w}_d + p w_d)}{C_1 \tanh[\mu(\dot{w}_d + p w_d)] + C_3(\dot{w}_d + p w_d)} \tag{3.3}$$

When the hysteresis is neglected $(p = 0)$ Eq. (3.3) is reduced to the form

$$I = \frac{F_d - C_2 \tanh(\mu \dot{w}_d) - C_4 \dot{w}_d}{C_1 \tanh(\mu \dot{w}_d) + C_3 \dot{w}_d} \tag{3.4}$$

4. Control system design

The main purpose of the considered control algorithm is to ensure that the MR damper should emulate operation of a viscous damper with the desired value of the viscous damping coefficient (c_{des}). It is assumed that the force generated by the controlled MR damper should be proportional to piston velocity (unlike in the passive mode of damper operation when the force depends on velocity in a minor degree only). For the given cable parameters, vibration mode and damper location, the desired viscous damping coefficient should be derived from Eq. (2.1) to ensure the maximal damping. A simplified diagram of the control algorithm is shown in Fig. 4.

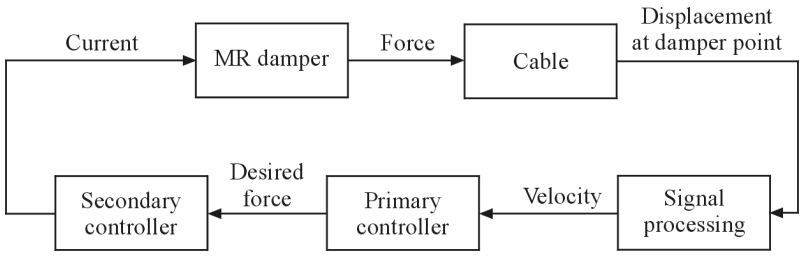

Fig. 4. A simplified diagram of the control algorithm

The algorithm utilises the feedback loop from the piston velocity. The velocity, in real conditions, might be reconstructed from the acceleration or piston displacement signals. For the purpose of the research program, the velocity signal was estimated on-line (*Signal Processing*) on the basis of piston displacement measurements. Knowing the velocity, the desired force is obtained (*Primary controller*), which is processed with the force tracking control system (*Secondary controller*) to obtain the current applied to the damper.

The major task in the implementation of the control algorithm is to ensure a satisfactory accuracy of the MR damper force tracking control. Damping force control might be handled either by applying an internal feedback from

the damper force or with no force feedback, by applying an inverse model of the damper. The second approach is adopted throughout this study. The inverse model of the damper, proposed in Subsection 3.2, is applied to the force tracking control system. The piston velocity and desired force are fed to the model input. The model output is a current which should ensure the desired damping force.

When the inverse model of the MR damper is employed, its accuracy is of key importance in the whole considered range of the piston velocity and current. However, degradation of force tracking capabilities might be caused by a phase shift in the feedback loop.

5. Experiments

5.1. Experimental setup

Experimental tests were run in a laboratory setup specially designed for the purpose of testing vibration reduction systems of a cable with MR dampers (Sapiński *et al.*, 2006). A diagram of the experimental setup and a photo of the MR damper installation are shown in Fig. 5 and Fig. 6.

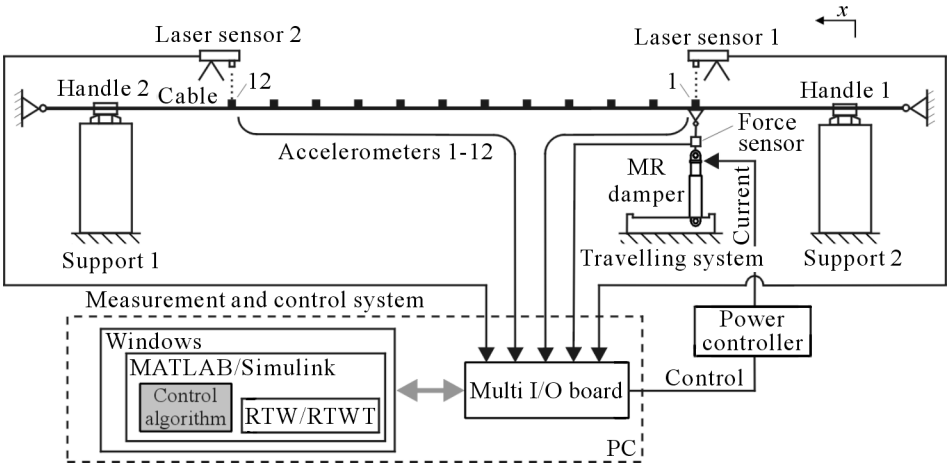

Fig. 5. A diagram of the experimental setup

There is a horizontally suspended steel cable, clamped at the ends. The length of the control section is $L = 30\,\mathrm{m}$, cable mass per unit length is $m = 1.8\,\mathrm{kg/m}$. The cable is tensioned using a lever mechanism. The maximum tension force approaches 50 kN. An MR damper of the RD-1097-01 type

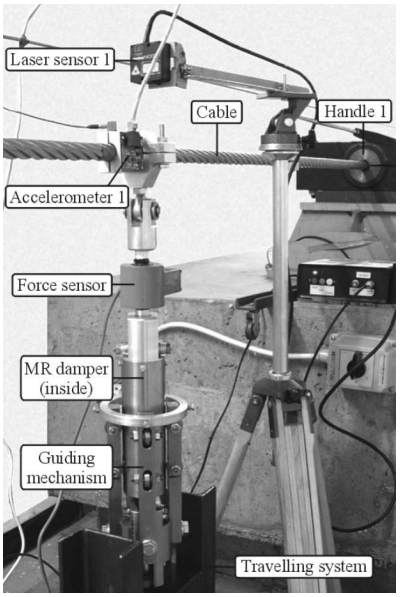

Fig. 6. A photograph of the MR damper installation

is attached near one of the cable supports. The damper is slide-mounted which allows one to investigate its performance at various positions determined by its distance from the support $(1, 2.5)$ m.

The measurement and control system comprises a PC with multi I/O board and MATLAB/Simulink. Transverse cable accelerations can be measured at maximally 12 locations, transverse cable displacements are measured at two points and the damper force is measured along the damper axis. The MR damper is controlled using a power controller operating in the analogue, voltage input – current output mode (Rosół and Sapiński, 2006).

On account of the adopted MR damper control algorithm, optimal values of viscous damping coefficients have to be estimated for given parameters of the facility. For the given cable parameters $(L,\ m)$, the optimal viscous damping coefficient depends on the static tension force T, damper attachment location x_d and the cable vibration mode. The tension force is taken to be 27 kN and $x_d = 1$ m, yielding c_{opt} of about 2100 Ns/m for the first mode, 1050 Ns/m for the second mode and 700 Ns/m for the third one. The force range of the RD-1097-01 MR damper allows the optimal viscous damper force to be tracked only in a certain amplitude range for the given mode (Fig. 7).

The results presented in this study apply to the first mode of free vibration. The chief advantage of the free vibration test is that the basic analysis of

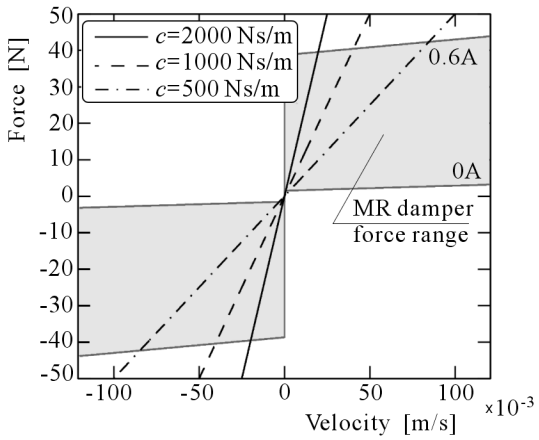

Fig. 7. Force-velocity characteristics for various linear viscous dampers in comparison to the MR damper (RD-1097-01) force range

registered data reveals relationships of damping and frequency as functions of the amplitude. Such observations are of primary importance in the analysis of dynamic properties of cables with MR dampers.

5.2. Cable with no damper

Free vibration measurement data are compiled in Fig. 8. There is no damper attached to the cable. The only measured quantity is displacement at the cable mid-point. The time when free vibration began is denoted as t_s. In the time range $(0,\, t_s)$ the cable was excited manually at the cable mid-point.

Cable vibration frequency and the modal damping ratio are identified basing on the analysis of the displacement envelope, yielding relationships between the amplitude, frequency and damping ratio (Figs. 8b and 8c). Dynamic component of the cable tension force increases with the amplitude, which is revealed as a slight increase in the free vibration frequency (Fig. 8b). The damping ratio for the first mode varies from $0.2 \cdot 10^{-3}$ for the amplitude $5 \cdot 10^{-3}$ m, to $1.05 \cdot 10^{-3}$ for the amplitude $80 \cdot 10^{-3}$ m. The obtained relationship between the damping ratio and amplitude is approximately linear in the investigated range.

5.3. Cable with MR damper in passive mode

Selected results of measurements of the vibration decay are shown in Fig. 9 and Fig. 10. Of particular interest is the first mode of free vibration of the

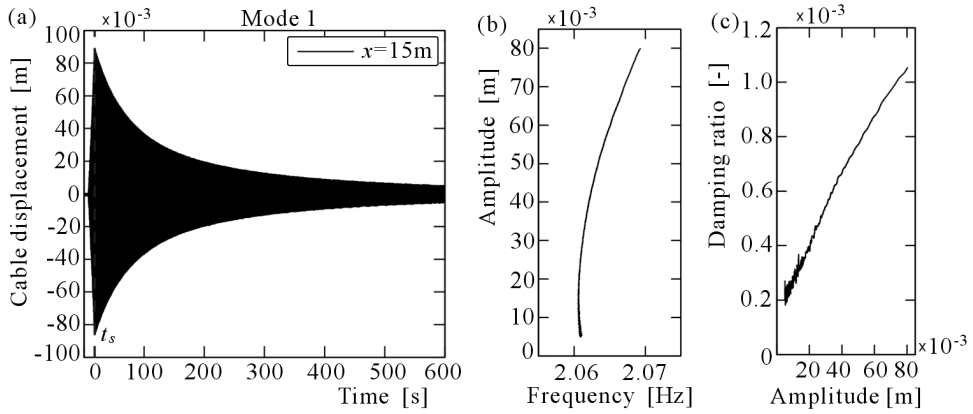

Fig. 8. Free vibration of a cable with no damper: (a) displacement decay at the cable mid-point, (b) relationship between the amplitude and frequency, (c) damping ratio vs. amplitude

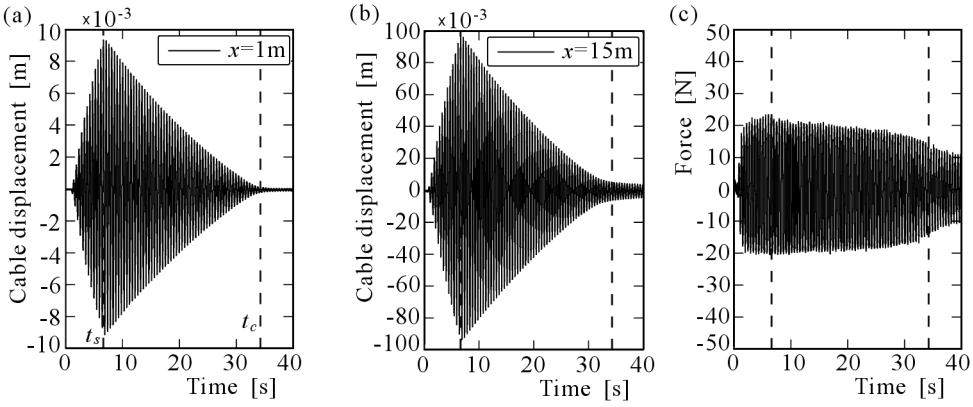

Fig. 9. Free vibration of the cable with the MR damper for $I = 0.25$ A: (a) cable displacement at the damper location, (b) cable displacement at the mid-point, (c) force along the damper axis

cable with the MR damper operating in the passive mode. The damper location is defined by the coordinate $x_d = 1$ m and two values of the applied current are considered: 0.25 A and 0.5 A. The measured quantities are: cable displacement and acceleration at the point the damper is attached, mid-point cable displacement and the force acting along the damper axis.

Free vibration of the cable with the attached damper tends to decay much faster than in the case of a cable with no damper as shown in Subsection 5.2. One has to bear in mind, however, that the decay is accompanied by a mi-

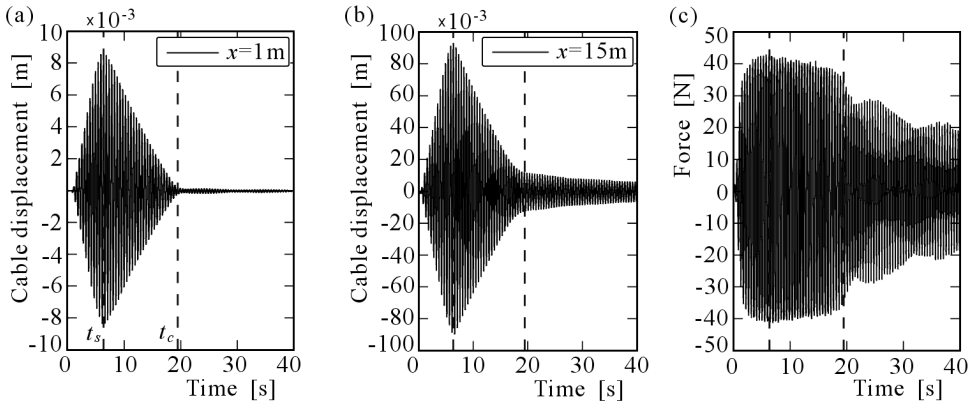

Fig. 10. Free vibration of the cable with the MR damper for $I = 0.5$ A: (a) cable displacement at the damper location, (b) cable displacement at the mid-point, (c) force along the damper axis

nor variation of the damper force amplitude (Fig. 9c and Fig. 10c). This very feature of the MR damper force leads to an adverse blocking effect of piston movement in the MR damper.

A rapid decay of cable vibration (the higher the current, the faster the vibration decay) is observed from the time when free vibration begins right till the moment when complete blocking of the MR damper occurs (denoted as t_c in Figs. 9 and 10). The damper blocking is observed when a force of cable action upon the damper is less than the force required to change the piston position in the whole period of vibration. As the vibration amplitude decays, the force of cable action upon the damper is reduced whilst the current-dependent friction component of the damper restoring force (F_c) remains unchanged. Comparison of these two forces allows for formulating a theoretical condition of the MR damper blocking (Weber *et al.*, 2005a; Maślanka, 2006). Graphs of cable displacements at the damper location and at the mid-point (Figs. 9a,b and 10a,b) indicate that when the damper stops working, the remaining part of the cable still vibrates with no appreciable damping. The point where the damper is attached becomes a node of a new, undamped mode with a slightly higher frequency. The observed frequency shift is accompanied by minor beating phenomenon revealed in the measured force (Fig. 10c).

MR damper characteristics describing the damper force as a function of piston velocity for the considered current are shown in Fig. 11. They are obtained in the time range from the 5th to 10th period of free vibration. The damper force is determined from force measurements along the damper axis (Figs. 9c and 10c). Presented force-velocity characteristics are well captured

by the damper model with hysteresis (Eq. (2.3)). The inertial force component, associated with the mass of damper attachment elements, has been subtracted.

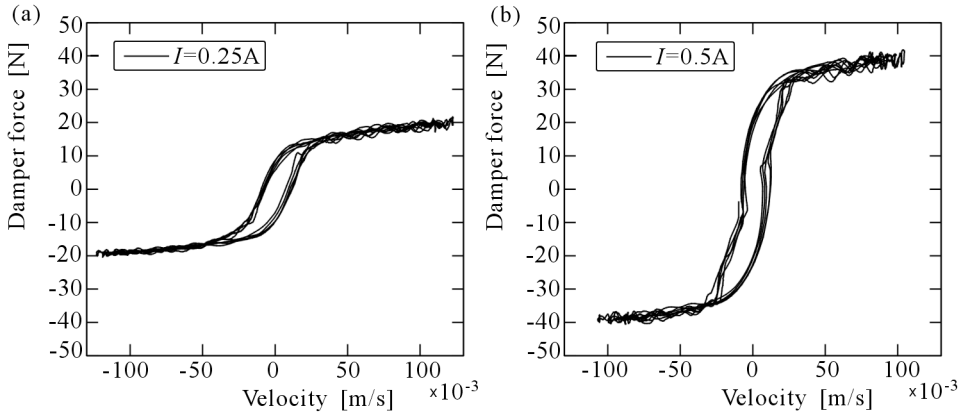

Fig. 11. Damper force vs. velocity for: (a) $I = 0.25\,\mathrm{A}$, (b) $I = 0.5\,\mathrm{A}$

The study of cable vibration with the MR damper in a passive mode involves analysis of the equivalent viscous damping coefficient. For a given damper restoring force (F_d) and piston velocity $(\dot{w}_d)$, the energy dissipated during one period of vibration (T_0) is equal to

$$\Delta E = \int_{t}^{t+T_0} F_d \dot{w}_d \, dt \tag{5.1}$$

Assuming that the displacement w_d is described by a sine function with an amplitude A, the same amount of energy per cycle shall be dissipated by a viscous damper with the equivalent viscous damping coefficient

$$c_{eq} = \Delta E \frac{T}{2\pi^2 A^2} \tag{5.2}$$

Figure 12a compiles the computed equivalent viscous damping coefficient c_{eq} obtained on the basis of measurements of the free vibration decay of the cable with the MR damper under the current 0.5 A. The calculation procedure is defined by Eqs. (5.1) and (5.2). The amplitude A is estimated by an envelope of the cable displacement signal at the point x_d. The velocity $\dot{w}_d$ is estimated on the basis of the cable acceleration signal measured at the point x_d. The obtained results are encumbered with a minor error only, because the velocity signal is close to the purely sine one. However, the lower the amplitude, the greater the error.

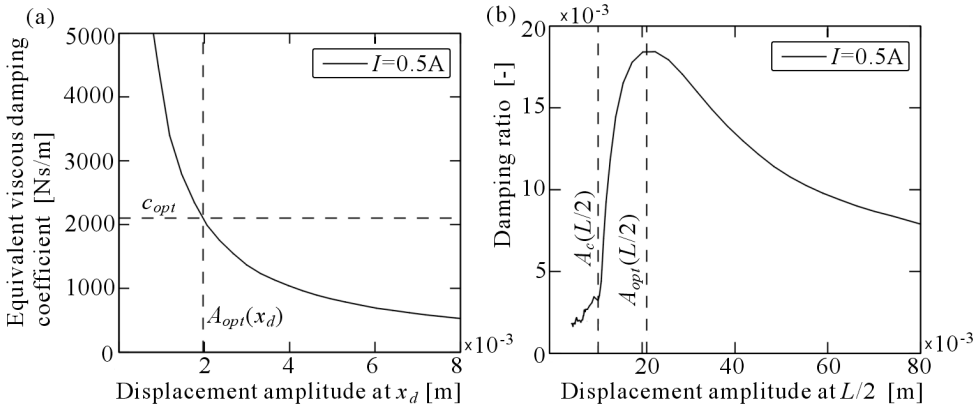

Fig. 12. Amplitude-dependent damping of the cable with the MR damper in the passive mode, $I = 0.5$ A: (a) equivalent viscous damping coefficient, (b) damping ratio

The coefficient c_{eq} is strongly dependent on the amplitude. That is because various amplitudes of piston displacements are associated with similar values of damper force amplitudes (compare Figs. 10a and 10c).

Figure 12a shows the optimal viscous damping coefficient c_{opt} obtained for the 1st mode and given parameters of the laboratory setup. For the assumed current, the equivalent viscous damping coefficient c_{eq} is equal to c_{opt} for the amplitude denoted as $A_{opt}(x_d)$. When the amplitude exceeds $A_{opt}(x_d)$, the value of c_{eq} decreases, without providing the optimal damping. When the vibration amplitude is less than $A_{opt}(x_d)$, the value of c_{eq} sharply increases and, finally, the cable gets clamped at the point the damper is attached.

A thorough analysis of Fig. 12b allows for interpretation of properties of cable vibration damping using an MR damper in the passive mode. This graph is plotted on the basis of the displacement signal measured at the cable midpoint. Damping ratio values are obtained in a narrow time window shifted along the time axis.

The damping curve in Fig. 12b has the maximum for the amplitude denoted as $A_{opt}(L/2)$. This amplitude is registered when c_{eq} equals approximately c_{opt} (Fig. 12a). When the amplitude of cable vibration is larger than $A_{opt}(L/2)$, the damping performance is lower. When the amplitude is less than $A_{opt}(L/2)$, the damping ratio of the cable assumes lower values. This is a consequence of getting closer to the blocking of the damper piston.

The amplitude denoted as $A_c(L/2)$ (see Fig. 12b) corresponds to the fully blocked damper. The MR damper when blocked does not dissipate the energy of cable vibration. That is why, for vibration amplitudes less than $A_c(L/2)$, the damping is minimal, approximately on the level of the cable internal damping.

It has to be emphasised that, for practical purposes, the characteristics in Fig. 12 seem very unfavourable. There is an obvious need to provide MR damper control in the vibration reduction system. The control should ensure that variations of vibration amplitudes should not produce any major deterioration of vibration damping performance.

5.4. Cable with MR damper in controlled mode

Figure 13 compiles measurement data collected for the first mode of free vibration of the cable with the MR damper controlled in accordance with the algorithm presented in Section 4. The damper location is given by the coordinate $x_d = 1\,\mathrm{m}$. The results are obtained for $c_{des} = 500\,\mathrm{Ns/m}$.

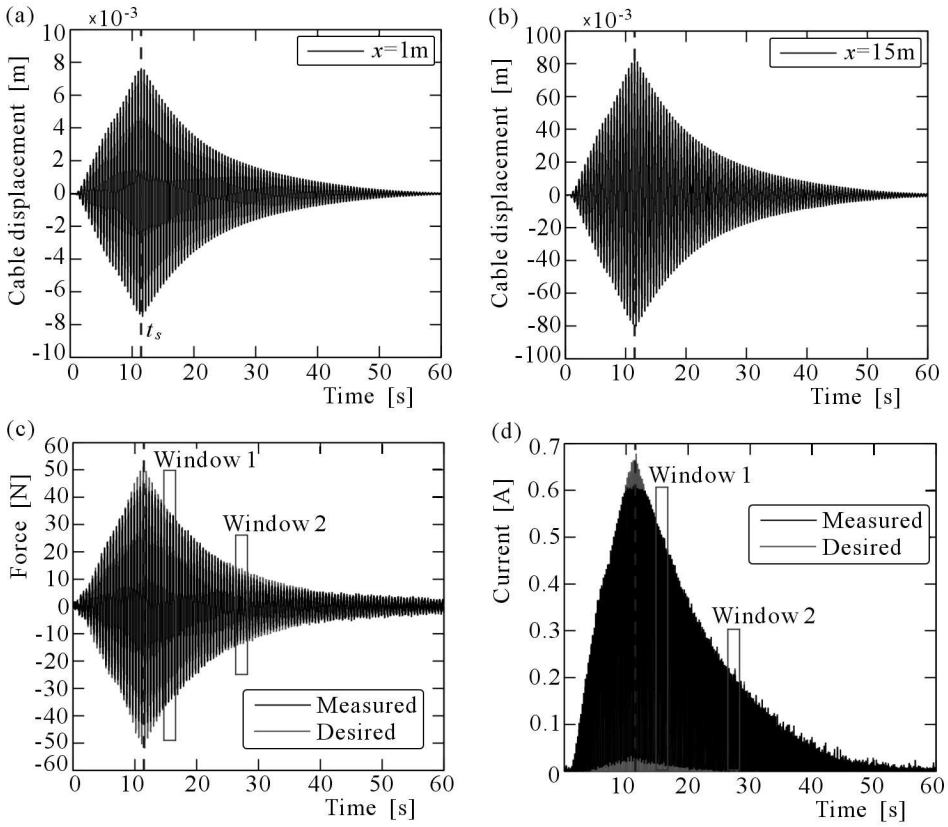

Fig. 13. Free vibration of the cable with the feedback controlled MR damper, $c_{des} = 500\,\mathrm{Ns/m}$: (a) cable displacement at the damper location, (b) cable displacement at the cable mid-point, (c) force along the damper axis, (d) current

Vibration decay plots shown in Fig. 13 vastly differ from cable vibration decay patterns collected when the damper was operating in the passive mode. The vibration decay envelope has a shape similar to an exponential curve. Furthermore, the displacement decay at the point the damper is attached (Fig. 13a) and at the cable mid-point (Fig. 13b) proceeds in the same manner throughout the whole considered amplitude range. Application of the control algorithm allowed the damper blocking effect to be almost entirely eliminated. The system comprising a cable with a controlled MR damper exhibits properties of a viscous-damped system, as planned.

Figure 13c compiles the force measured along the damper axis and the desired force proportional to piston velocity. The MR damper force was generated by the current, plotted in Fig. 13d. At maximum cable displacements, the desired force determined by the control algorithm is slightly higher than the maximum force to be generated by the MR damper RD-1097-01. Hence the observed difference between the two forces in this interval. This also applies to the difference between the current levels: that required to produce the desired force and the measured one.

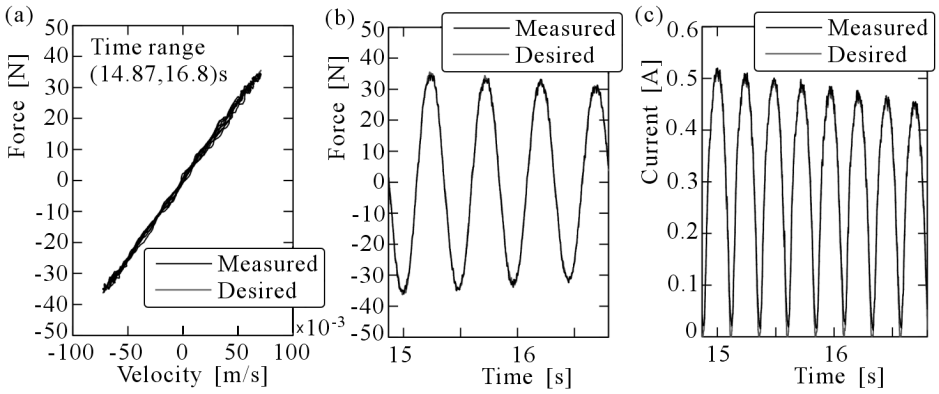

Fig. 14. Illustration of force tracking control accuracy, $c_{des} = 500\,\mathrm{Ns/m}$: (a) force vs. velocity, (b) force acting along the damper axis (zoomed window 1 of Fig. 13c), (c) current (zoomed window 1 in Fig. 13d)

Tracking accuracy of the MR damper force is presented in more detail for two selected time intervals. The first one (Fig. 14) covers subsequent free vibration periods (from 8 to 12) designated as window 1 in Fig. 13. The error of the desired force representation is minimal in this interval. The other interval covers free vibration periods 32-36 (window 2). The force tracking error in this range takes the maximum value.

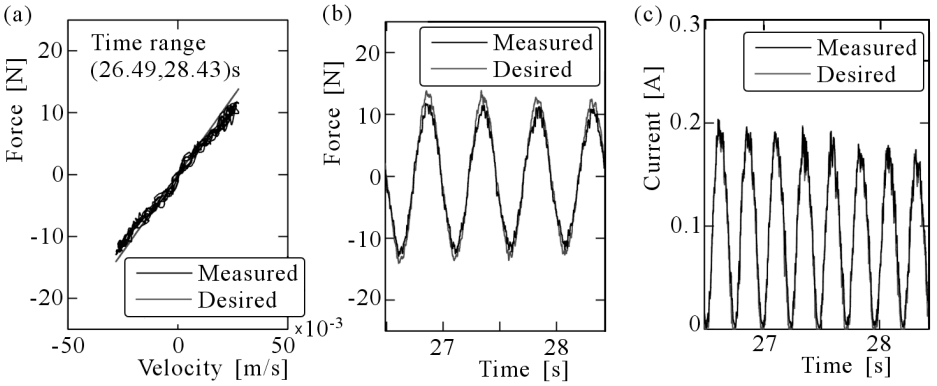

Fig. 15. Illustration of force tracking control accuracy, $c_{des} = 500\,\mathrm{Ns/m}$: (a) force vs. velocity, (b) force acting along the damper axis (zoomed window 2 in Fig. 13c), (c) current (zoomed window 2 in Fig. 13d)

Force-velocity relationships are given for these two considered time intervals. There are also plots of the force and applied current in function of time. The measured data are compared with the desired values generated by the control system. Plots in Fig. 14 and Fig. 15 confirm the adequacy of the applied control algorithm. When the appropriate control algorithm is adopted, the MR damper well emulates a linear viscous damper with the given operational characteristics. The resultant force-velocity relationship is similar to the desired characteristic and does not exhibit any hysteresis typical for MR dampers operating in the passive mode (Fig. 11). The force tracking error observed in Figs. 15a and 15b results from the fact that the relationships between the damper model parameters and the applied current are approximated by a linear function (Fig. 3). In the current interval where the approximation error was the largest $(0.1, 0.2)\,\mathrm{A}$, the force tracking error would be maximal, too.

It is worthwhile to mention that underlying the experiments was the inverse model of an MR damper with no hysteresis (Eq. (3.4)). As the force tracking control accuracy is satisfactory, the application of the inverse model with hysteresis does not seem justified.

Figure 16a shows the equivalent viscous damping coefficient (c_{eq}) derived from Eqs. (5.1) and (5.2). In an ideal case, the value c_{eq} should be equal to the desired value c_{des}, no matter what amplitude. In our case, for amplitudes larger than $7 \cdot 10^{-3}\,\mathrm{m}$, the observed difference between c_{eq} and c_{des} is a consequence of the maximum force constraints in the MR damper. For amplitudes lower than $10^{-3}\,\mathrm{m}$, current stabilises on $0\,\mathrm{A}$, a further amplitude decay will not produce the desired reduction of the damper force (see Fig. 13), which corresponds to increase of c_{eq} in this interval, in accordance with Eq. (5.2).

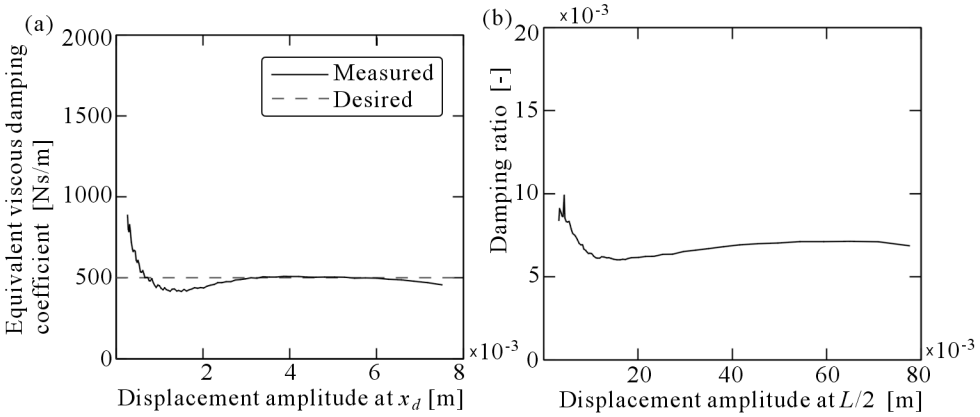

Fig. 16. Amplitude-dependent damping for the cable with the feedback controlled MR damper, $c_{des} = 500\,\mathrm{Ns/m}$: (a) equivalent viscous damping coefficient, (b) damping ratio

Figure 16b gives a plot of the cable damping ratio obtained on the basis of the mid-point cable displacement signal. This characteristic is associated with that in Fig. 16a and takes a fixed value $(6 \cdot 10^{-3}, 8 \cdot 10^{-3})$ in a wide range of amplitudes. The obtained damping level corresponds to the desired value c_{des}. The considered value of the desired viscous damping coefficient $c_{des} = 500\,\mathrm{Ns/m}$ makes up for about 25% of the optimal damping level.

6. Discussion of obtained results

The research data compiled in this study are achieved for the first mode of free vibration and damper position defined by the coordinate $x_d = 1\,\mathrm{m}$. The measurement data obtained for the cable with an attached MR damper operating in the passive mode are summarised in Subsection 5.3, for two values of current. The assumed value of the desired viscous damping coefficient $c_{des} = 500\,\mathrm{Ns/m}$ is about 25% of the optimal value for the first mode.

The laboratory tests were conducted for various current levels from the range $(0, 0.5)\,\mathrm{A}$ and for several values of desired viscous damping coefficients, ranging from 100 to 2000 Ns/m. The obtained data became the starting point for comparative analysis of cable vibration damping using MR dampers in the two operating modes. The applied criterion is the rate of vibration decay, as used by Weber *et al.* (2005a). The mid-point displacement signal is utilised to find the time necessary to decay of preset percentage fraction of the initial

amplitude. The assumed factor $t_{90\%}$ determines the time required for 90% decay of the initial amplitude.

Figure 17a shows a plot of the decay time versus the current applied to the MR damper. This relationship has a minimum at 0.4 A. At current levels exceeding 0.4 A, the decay time tends to increase due to the damper blocking effect. In terms of the assumed criterion, the current 0.4 A appears to be optimal. The value of the decay time $t_{90\%}$ is 16 s for this current.

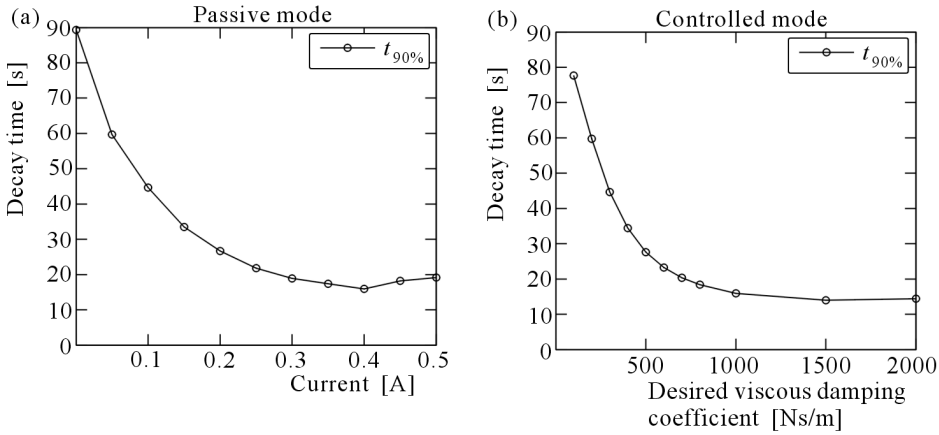

Fig. 17. Free vibration decay time for the cable with the attached MR damper, $x_d = 1$ m: (a) passive mode, (b) controlled mode

Figure 17b shows a plot of the decay time obtained from measurements of cable vibration with a controlled damper. Values of $t_{90\%}$ are given in function of the desired viscous damping coefficient c_{des}. The minimum value of the decay time $t_{90\%}$ (achieved for $c_{des} = 2000$ Ns/m) is equal to 14 s.

A comparison of plots in Figs. 17a and 17b does not reveal major improvements of the vibration reduction performance when the control algorithm is applied. It has to be emphasised, however, that for c_{des} exceeding 500 Ns/m, the damping force tracking involves a certain error due to the fact that no larger force can be realized than the maximum force of the MR damper used in the study. For example, for $c_{des} = 2000$ Ns/m, the maximum value of the desired force is 220 N, whilst the force generated by the MR damper approaches 45 N. For the given c_{des}, the error is greater for higher amplitudes. The plot in Fig. 17b does not fully portray the cable vibration damping capacity for the adopted control algorithm. When the MR damper is capable of generating larger forces, the decay time should take lower values.

The decay time of the cable with no damper equals $t_{90\%} = 400\,\mathrm{s}$ (Fig. 8a). Connecting the damper at the point $x_d = 1\,\mathrm{m}$ allows for approximately 25-fold (passive mode) and 28-fold (controlled mode) reduction of the time needed to decay 90% of the initial amplitude for the first mode of free vibration.

7. Summary

The paper compiles the results of laboratory testing of a cable vibration reduction system complete with an MR damper. Damper operation was investigated both in the passive and controlled mode.

Measurements taken on the cable with the damper operating in the passive mode reveal strongly nonlinear properties of the system. The main source of nonlinearity is the MR damper.

The analysis of damping of the cable-damper system utilises an equivalent viscous damping and a non-dimensional damping ratio. Results of analysis justify the need to implement an appropriate algorithm to control the MR damper to ensure the desired damping level (independent of amplitude).

The paper outlines the implementation of the algorithm based on a feedback loop from the piston velocity. The control system structure comprises a primary controller with the desired damping force as the output and a secondary controller to control the MR damper force. Application of an MR damper inverse model in the force control system ensures sufficient precision of control without a need of another feedback loop from the damper force. The inverse model was created on the basis of the MR damper model with linear approximations of relationships between the model parameters and the applied current. It has to be pointed out that in the case of MR dampers, where the relationship between the model parameters and the current is nonlinear, this approach might lead to major errors. Delays in the measurement and control system are the source of an additional error in the force tracking control.

Results of measurements of free vibration of a cable with an attached controlled MR damper confirm the adequacy of algorithm implementation. The analysis of measurement data indicates that an appropriately controlled damper ensures a nearly constant damping level in a wide range of amplitudes, which is a major benefit of viscous dampers. However, the maximal, theoretically predicted damping level is impossible to achieve during the experiments. These constraints are associated with the limited force range of the MR damper used in the tests.

It is worthwhile to mention that the investigated control concept might be implemented in an alternative manner, by periodic changing of the current, depending on the vibration amplitude (Maślanka, 2008). The current is changed once per one period of vibration, in response to the instantaneous amplitude of the piston displacement and vibration frequency. The thus achieved cable damping performance is similar to that reported in this study.

Acknowledgements

The work is supported by the State Committee for Scientific Research (Poland) as a part of the research program No. 4 T07B 008 30.

References

1. AIM, 2005, *Proceedings of the 6th International Symposium on Cable Dynamics*, Charleston, USA, September 19-22

2. CARLSON J.D., 1999, Low-cost MR fluid sponge devices, *Journal of Intelligent Material Systems and Structures*, **10**, 8, 589-594

3. CHEN Z.Q., WANG X.Y., KO J.M., NI Y.Q., SPENCER B.F. JR., YANG G., 2003, MR damping system on Dongting Lake cable-stayed bridge, *Smart Structures and Materials 2003: Smart Systems and Nondestructive Evaluation for Civil Infrastructures*, Liu S.C. (Edit.), *Proceedings of SPIE*, **5057**, 229-235

4. CHRISTENSON R.E., SPENCER B.F. JR, JOHNSON E.A., 2001, Experimental verification of semiactive damping of stay cables, *Proceedings of the 2001 American Control Conference*, Arlington, USA, June 25-27, 5058-5063

5. CHRZAN M.J., CARLSON J.D., 2001, MR fluid sponge devices and their use in vibration control of washing machines, *Smart Structures and Materials 2001: Damping and Isolation*, Inman D.J. (Edit.), *Proceedings of SPIE*, **4331**, 370-378

6. DU H., SZE K.Y., LAM J., 2005, Semi-active H_∞ control of vehicle suspension with magneto-rheological dampers, *Journal of Sound and Vibration*, **283**, 981-996

7. DUAN Y.F., NI Y.Q., KO J.M., 2005, State-derivative feedback control of cable vibration using semiactive magnetorheological dampers, *Computer-Aided Civil and Infrastructure Engineering*, **20**, 431-449

8. DUAN Y.F., NI Y.Q., KO J.M., 2006, Cable vibration control using magnetorheological dampers, *Journal of Intelligent Material Systems and Structures*, **17**, 4, 321-325

9. EMPA, 2006, Preventing bridges from oscillating – premiére in Dubrovnik, Press release, Duebendorf / St. Gallen, Switzerland, July 26, http://www.empa.ch

10. GANDHI F., BULLOUGH W.A., 2005, On the phenomenological modeling of electrorheological and magnetorheological fluid preyield behavior, *Journal of Intelligent Material Systems and Structures*, **16**, 3, 237-248

11. GONCALVES F.D., KOO J.H., AHMADIAN M., 2006, A review of the state of the art in magnetorheological fluid technologies – part I: MR fluid and MR fluid models, *The Shock and Vibration Digest*, **38**, 3, 203-219

12. GUO S., YANG S., PAN C., 2006, Dynamic modeling of magnetorheological damper behaviors, *Journal of Intelligent Material Systems and Structures*, **17**, 1, 3-14

13. HIKAMI Y., SHIRAISHI N., 1988, Rain-wind induced vibrations of cables in cable-stayed bridges, *Journal of Wind Engineering and Industrial Aerodynamics*, **29**, 409-418

14. JOHNSON E.A., BAKER G.A., SPENCER B.F. JR., FUJINO Y., 2000, Mitigating stay cable oscillation using semiactive damping, *Smart Structures and Materials 2000: Smart Systems for Bridges, Structures, and Highways*, Liu S.C. (Edit.), *Proceedings of SPIE*, **3988**, 207-216

15. JOHNSON E.A., CHRISTENSON R.E., SPENCER B.F. JR., 2003, Semiactive damping of cables with sag, *Computer-Aided Civil and Infrastructure Engineering*, **18**, 132-146

16. JOHNSON E.A., SPENCER B.F. JR., FUJINO Y., 1999, Semiactive damping of stay cables: a preliminary study, *Proceedings of the 17th International Modal Analysis Conference*, Society for Experimental Mechanics, Bethel, USA, 417-423

17. JOLLY M. R., BENDER J. W., CARLSON J. D., 1999, Properties and applications of commercial magnetorheological fluids, *Journal of Intelligent Material Systems and Structures*, **10**, 1, 5-13

18. KRENK S., 2000, Vibrations of a taut cable with an external damper, *Journal of Applied Mechanics, ASME*, **67**, 772-776

19. KUMARASENA S., JONES N.P., IRWIN P., TAYLOR P., 2005, Wind induced vibration of stay cables, *FHWA/HNTB Interim Final Report No. RI98-034*, National Technical Information Center, Springfield, USA

20. KWOK N.M, HA Q.P., NGUYEN T.H., LI J., SAMALI B., 2006, A novel hysteretic model for magnetorheological fluid dampers and parameter identification using particle swarm optimization, *Sensors and Actuators A*, **132**, 441-451

21. LARSEN A., LAFRENIÉRE A., 2005, Application of a limit cycle oscillator model to bridge cable galloping, *Proceedings of the 6th International Symposium on Cable Dynamics*, Charleston, USA, September 19-22, on CD

22. Lord Co., 2002, RD-1097-01 Product Bulletin, http://www.lord.com

23. MAIN J.A., JONES N.P., 2001, Evaluation of viscous dampers for stay-cable vibration mitigation, *Journal of Bridge Engineering, ASCE*, **6**, 6, 385-397

24. MAŚLANKA M., 2006, About clamping phenomenon of a taut cable with an attached MR damper, *Vibrations in Physical Systems*, **XXII**, Cempel C., Stefaniak J. (Edit.), Poznan University of Technology, Poznan, Poland, 265-271

25. MAŚLANKA M., 2008, *Semiaktywny układ redukcji drgań liny z tłumikiem magnetoreologicznym*, Ph.D. Disseration, AGH University of Science and Technology, Cracow, Poland (in progress)

26. MoDOT – Missouri Department of Transportation, 2006, *2nd Workshop on Wind Induced Vibration of Cable Stay Bridges*, St. Louis, USA, April 25-27, http://www.modot.org/csb

27. PERSOON A.J., NOORLANDER K., 1999, Full-scale measurements on the Erasmus Bridge after rain/wind induced cable vibrations, *Proceedings of the 10th International Conference on Wind Engineering*, Copenhagen, Denmark, June 21-24, 1019-1026

28. ROSÓŁ M., SAPIŃSKI B., 2006, Dynamics of a magnetorheological damper driven by a current driver, *Proceedings of the 12th IEEE International Conference on Methods and Models in Automation and Robotics*, Miedzyzdroje, Poland, August 28-31, 423-428

29. SAPIŃSKI B., SNAMINA J., MAŚLANKA M., ROSÓŁ M., 2006, Facility for testing of magnetorheological damping systems for cable vibrations, *Mechanics*, AGH University of Science and Technology Press, **25**, 3, 135-142

30. SAVOR Z., RADIC J., HRELJA G., 2006, Cable vibrations at Dubrovnik bridge, *Bridge Structures*, **2**, 2, 97-106

31. SPENCER B.F. JR., DYKE S.J., SAIN M.K., CARLSON J.D., 1997, Phenomenological model of a magnetorheological damper, *Journal of Engineering Mechanics, ASCE*, **123**, 3, 230-238

32. SUN L., ZHANG Q., CHEN A., LIN Z., 2004, Cable vibration control countermeasures and structural health monitoring system design of Sutong Bridge, *Proceedings of the 2nd International Conference on Bridge Maintenance, Safety and Management*, Kyoto, Japan, October 18-22

33. TSANG H.H., SU R.K.L., CHANDLER A.M., 2006, Simplified inverse dynamics models for MR fluid dampers, *Engineering Structures*, **28**, 327-341

34. VIRLOGEUX M., 1999, Recent evolution of cable-stayed bridges, *Engineering Structures*, **21**, 737-755

35. VIRLOGEUX M., 2005, State-of-the-art in cable vibrations of cable-stayed bridges, *Bridge Structures*, **1**, 3, 133-168

36. WEBER F., DISTL H., FELTRIN G., MOTAVALLI M., 2005a, Simplified approach of velocity feedback for MR dampers on real cable-stayed bridges, *Proceedings of the 6th International Symposium on Cable Dynamics*, Charleston, USA, September 19-22, on CD

37. WEBER F., DISTL H., NÜTZEL O., 2005b, Versuchsweiser Einbau eines adaptiven Seildämpfers in eine Schrägseilbrücke, *Beton- und Stahlbetonbau*, **100**, 7, 582-589

38. WEBER F., FELTRIN G., MOTAVALLI M., 2005c, Measured linear-quadratic-Gaussian controlled damping, *Smart Materials and Structures*, **14**, 1172-1183

39. WEBER F., FELTRIN G., MOTAVALLI M., 2005d, Passive damping of cables with MR dampers, *Materials and Structures*, **38**, 568-577

40. WU W.J., CAI C.S., 2006, Experimental study of magnetorheological dampers and application to cable vibration control, *Journal of Vibration and Control*, **12**, 1, 67-82

41. XIA P.Q., 2003, An inverse model of MR damper using optimal neural network and system identification, *Journal of Sound and Vibration*, **266**, 1009-1023

42. ZHOU H., SUN L., 2005, A full-scale cable vibration mitigation experiment using MR damper, *Proceedings of the 6th International Symposium on Cable Dynamics*, Charleston, USA, September 19-22, on CD

Badania eksperymentalne sterowania drganiami liny z dołączonym tłumikiem MR

Streszczenie

W artykule przedstawiono wyniki badań eksperymentalnych układu poziomo zawieszonej liny z tłumikiem MR dołączonym poprzecznie w pobliżu podpory. Do sterowania tłumikiem MR przyjęto koncepcję emulacji tłumika wiskotycznego o optymalnym współczynniku tłumienia. Algorytm sterowania zrealizowano przy wykorzystaniu sprzężenia od prędkości oraz nadążnego układu sterowania siłą tłumienia. Analizie poddano drgania swobodne liny z tłumikiem MR pracującym w trybie pasywnym oraz sterowanym. Wyniki badań wskazują, że opracowany algorytm sterowania pozwala na uzyskanie w przybliżeniu stałego poziomu tłumienia drgań liny w szerokim zakresie wartości amplitudy drgań.

Manuscript received March 26, 2007; accepted for print July 4, 2007